

## Metrological Detection of Multipartite Entanglement from Young Diagrams

Zhihong Ren<sup>1,2</sup>, Weidong Li<sup>1,\*</sup>, Augusto Smerzi<sup>1,3,†</sup> and Manuel Gessner<sup>2,‡</sup>

<sup>1</sup>*Institute of Theoretical Physics and Department of Physics, State Key Laboratory of Quantum Optics and Quantum Optics Devices, Collaborative Innovation Center of Extreme Optics, Shanxi University, Taiyuan 030006, China*

<sup>2</sup>*Laboratoire Kastler Brossel, ENS-Université PSL, CNRS, Sorbonne Université, Collège de France, 24 Rue Lhomond, 75005 Paris, France*

<sup>3</sup>*QSTAR, INO-CNR, and LENS, Largo Enrico Fermi 2, 50125 Firenze, Italy*



(Received 7 December 2020; accepted 13 January 2021; published 25 February 2021)

We characterize metrologically useful multipartite entanglement by representing partitions with Young diagrams. We derive entanglement witnesses that are sensitive to the shape of Young diagrams and show that Dyson’s rank acts as a resource for quantum metrology. Common quantifiers, such as the entanglement depth and  $k$ -separability are contained in this approach as the diagram’s width and height. Our methods are experimentally accessible in a wide range of atomic systems, as we illustrate by analyzing published data on the quantum Fisher information and spin-squeezing coefficients.

DOI: [10.1103/PhysRevLett.126.080502](https://doi.org/10.1103/PhysRevLett.126.080502)

An efficient classification of entanglement in multipartite systems is crucial for our understanding of quantum many-body systems and the development of quantum information science [1–4]. A particular challenge is the development of experimentally implementable criteria for the detection of multipartite entanglement [5,6]. The development of quantum technologies further demands a precise understanding of the set of multipartite entangled states that enable a quantum advantage in specific applications of quantum information [7,8]. In this context, metrological entanglement criteria are powerful tools that establish a quantitative link between the number of detected entangled parties and the quantum gain in interferometric measurements [8–12].

As a consequence of the exponentially increasing number of partitions in multipartite systems, there is no unique way to quantify multipartite entanglement. Common approaches to capture the extent of multipartite correlations focus on simple integer indicators [5]: An entanglement depth of  $w$  describes that at least  $w$  parties must be entangled, while  $h$ -inseparability expresses that the system cannot be split into  $h$  separable subsystems. Larger values of  $w$  and smaller values of  $h$  generally indicate more multipartite entanglement, and experimentally observable bounds on both can be obtained with different methods [5,6], including from the metrological sensitivity in terms of the quantum Fisher information [11].

A systematic approach based on the partitions of a multipartite system reveals a duality between  $w$  and  $h$  [13]. Let us illustrate this with the example of a 7-partite system that allows for a separable description in the partition  $\Lambda = 1|2345|67$ , see Fig. 1. The system is separable into  $h = 3$  subsets and it contains entanglement among up to  $w = 4$  parties, i.e., it has an entanglement depth of  $w = 4$ . By using the correspondence between partitions of a system (up to

permutations of the particle labels) and Young diagrams, we can represent this partition as  $\Lambda \sim \begin{array}{|c|c|c|c|} \hline \square & \square & \square & \square \\ \hline \square & \square & & \\ \hline \square & & & \\ \hline \end{array}$ , where each box represents one party and each row represents an entangled subset of decreasing size from top to bottom. We can easily convince ourselves that  $w$  and  $h$  correspond to the width and height of the Young diagram, respectively.

Focusing exclusively on one of these two quantities provides only limited information about the allowed structure of separable partitions. The entanglement depth  $w$  refers to the size of the largest subset but ignores the size and number of the remaining subsets. For instance,  $w = 4$  does not distinguish between the partition  $\Lambda$  and, e.g.,  $\Lambda' \sim \begin{array}{|c|c|c|} \hline \square & \square & \square \\ \hline \square & \square & \\ \hline \square & & \\ \hline \end{array}$ , even though the latter clearly contains more entanglement. Separability, in contrast, is insensitive to the size of the entangled subsets and  $h = 3$  is also compatible with, e.g.,  $\Lambda'' \sim \begin{array}{|c|c|} \hline \square & \square \\ \hline \square & \square \\ \hline \square & \\ \hline \end{array}$ . As an alternative integer quantifier, the rank of a partition, defined by Dyson [14] as  $r = w - h$ , combines the information about  $w$  and  $h$ , and was recently suggested to express the “stretchability” of correlations [13]. In our example, it successfully distinguishes these

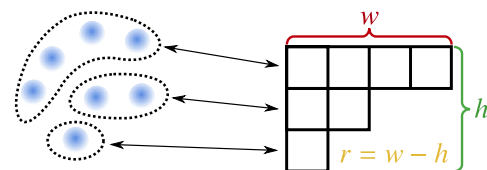


FIG. 1. Representation of multipartite entanglement using Young diagrams. In this example, a system of  $N = 7$  particles is separable in a partition into  $h = 3$  subsets and contains an entanglement depth of  $w = 4$  particles. These quantities correspond to height  $h$  and width  $w$  of the associated Young diagram. Dyson’s rank  $r = w - h$  combines both pieces of information.

partitions and yields the intuitive order  $r(\Lambda'') = 0$ ,  $r(\Lambda) = 1$ , and  $r(\Lambda') = 2$ . With  $2N - 3$  steps between fully separable and genuine  $N$ -partite entangled states,  $r$  provides a scale almost twice as fine as those provided by the  $N$  possible values of  $w$  and  $h$ , respectively.

In this Letter, we derive metrological entanglement criteria that provide combined information about  $w$  and  $h$ , or about Dyson's rank  $r$ . We base our criteria on quantifiers of metrological sensitivity that are widely used both in theory and experiments. Our results reveal hidden details about the structure of multipartite entanglement from the quantum Fisher information or spin-squeezing parameters, while relying only on established measurement techniques. This leads to a better understanding of metrologically useful multipartite entanglement, and uncovers in particular the role of  $r$  as a resource for quantum-enhanced metrology. As a single integer quantifier,  $r$  is found to provide most information about multipartite entanglement in the experimentally relevant regime of limited multipartite entanglement. The entanglement depth  $w$ , instead, is shown to be most effective close to genuine  $N$ -partite entanglement.

*Metrological witness for  $(w, h)$ -entanglement.*—We characterize the degree of multipartite entanglement in terms of the partitions that are compatible with a separable description of the correlations. A partition  $\Lambda = \{A_1, A_2, \dots, A_{|\Lambda|}\}$  separates the total  $N$ -partite system into  $|\Lambda|$  nonempty, disjoint subsets  $A_l$  of size  $N_l$  such that  $\sum_{l=1}^{|\Lambda|} N_l = N$ . A state  $\hat{\rho}_\Lambda$  is  $\Lambda$ -separable if there exist local quantum states  $\hat{\rho}_{A_l}^{(\gamma)}$  for each subsystem and a probability distribution  $p_\gamma$  such that  $\hat{\rho}_\Lambda = \sum_\gamma p_\gamma \hat{\rho}_{A_1}^{(\gamma)} \otimes \dots \otimes \hat{\rho}_{A_{|\Lambda|}}^{(\gamma)}$ . The partitions can be classified according to the number  $|\Lambda|$  of subsets and the size  $\max \Lambda = \max_l |A_l|$  of the largest subset, i.e., the respective height  $h$  and width  $w$  of the associated Young diagram. The entanglement depth is defined with respect to the set  $\mathcal{L}_{w\text{-prod}} = \{|\Lambda| \mid \max \Lambda \leq w\}$  of partitions with maximal width  $w$ . Any state that cannot be written as a  $w$ -producible state  $\hat{\rho}_{w\text{-prod}} = \sum_{\Lambda \in \mathcal{L}_{w\text{-prod}}} P_\Lambda \hat{\rho}_\Lambda$ , where  $P_\Lambda$  is a probability distribution, has an entanglement depth of at least  $w + 1$ . Analogously, inseparability is related to the set  $\mathcal{L}_{h\text{-sep}} = \{|\Lambda| \mid |\Lambda| \geq h\}$  of partitions with minimal height  $h$  and  $h$ -inseparable states cannot be represented in the form  $\hat{\rho}_{h\text{-sep}} = \sum_{\Lambda \in \mathcal{L}_{h\text{-sep}}} P_\Lambda \hat{\rho}_\Lambda$ . By combining both pieces of information, we obtain a finer description of multipartite quantum correlations by the set of  $(w, h)$ -entangled states, i.e., those that cannot be modeled as  $(w, h)$ -separable states

$$\hat{\rho}_{(w,h)\text{-sep}} = \sum_{\Lambda \in \mathcal{L}_{w\text{-prod}} \cap \mathcal{L}_{h\text{-sep}}} P_\Lambda \hat{\rho}_\Lambda. \quad (1)$$

To derive criteria that allow us to distinguish between different  $(w, h)$  classes, we derive the metrological sensitivity limits for states with restricted values of  $w$  and  $h$ . Measuring or calculating the sensitivity of a state then

allows us to put bounds on  $w$  and  $h$  by comparison with these limits. In the following we focus on  $N$ -qubit systems, described by collective angular momentum operators  $\hat{J}_\mathbf{n} = \sum_{i=1}^N \mathbf{n} \cdot \hat{\boldsymbol{\sigma}}^{(i)}/2$  with unit vector  $\mathbf{n} \in \mathbb{R}^3$  and  $\hat{\boldsymbol{\sigma}}^{(i)} = (\hat{\boldsymbol{\sigma}}_x^{(i)}, \hat{\boldsymbol{\sigma}}_y^{(i)}, \hat{\boldsymbol{\sigma}}_z^{(i)})$  a vector of Pauli matrices for the  $i$ th qubit. The central theorem of quantum metrology, the quantum Cramér-Rao bound  $(\Delta\theta_{\text{est}})^2 \geq 1/F_Q[\hat{\rho}, \hat{J}_\mathbf{n}]$ , defines the achievable precision limit for the estimation of a phase shift  $\theta$  generated by  $\hat{J}_\mathbf{n}$ , using the state  $\hat{\rho}$  [7,8,10,15,16]. The phase  $\theta$  is estimated from measurements of the quantum state  $\hat{\rho}(\theta) = \hat{U}(\theta)\hat{\rho}\hat{U}(\theta)^\dagger$  with  $\hat{U}(\theta) = e^{-i\hat{J}_\mathbf{n}\theta}$  and the quantum Fisher information  $F_Q[\hat{\rho}, \hat{J}_\mathbf{n}]$  describes the sensitivity of  $\hat{\rho}(\theta)$  to small variations of  $\theta$  [15]. As an experimentally accessible quantity,  $F_Q$  has been employed in the past as a versatile entanglement witness [2,4,8,9,11,17–19].

We are now in a position to present the main results of this work. The quantum Fisher information of any  $(w, h)$ -separable state is limited to

$$F_Q[\hat{\rho}_{(w,h)\text{-sep}}, \hat{J}_\mathbf{n}] \leq w(N - h) + N, \quad (2)$$

where  $N/h \leq w \leq N - h + 1$  and  $N/w \leq h \leq N - w + 1$ . The bound (2) can be slightly tightened by explicitly considering the division of  $N$  into integer subsets, and in this case it is saturated by an optimal quantum state. A detailed proof of Eq. (2) in its most general form, as well as the optimal states are provided in the Supplemental Material [20]. The monotonic growth of Eq. (2) in  $w$  and its monotonic decrease in  $h$  demonstrate that higher quantum advantages in metrology measurements require entanglement among larger sets of particles.

In the extreme cases where all or none of the parties are entangled, we recover the well-known limits of classical and quantum parameter estimation strategies, respectively [16]. Fully separable states, defined by  $(w, h) = (1, N)$ , are limited to  $F_Q[\hat{\rho}_{(1,N)\text{-sep}}, \hat{J}_\mathbf{n}] \leq F_{\text{SN}}[\hat{J}_\mathbf{n}] = N$ , which leads to shot-noise sensitivity  $(\Delta\theta_{\text{est}})^2 \geq 1/N$ , while genuine  $N$ -partite entanglement,  $(w, h) = (N, 1)$ , enables sensitivities up to the Heisenberg limit  $F_Q[\hat{\rho}_{(N,1)\text{-sep}}, \hat{J}_\mathbf{n}] \leq N^2$  with  $(\Delta\theta_{\text{est}})^2 \geq 1/N^2$  [8–10]. In between these extreme cases, the metrological potential of finitely entangled states is captured by the combined information provided by the tuple  $(w, h)$ . The metrological entanglement witness (2) has a particularly simple interpretation: It identifies the quantum advantage offered by  $(w, h)$ -entanglement in terms of the sensitivity difference to the shot-noise limit,  $Q[\hat{\rho}, \hat{J}_\mathbf{n}] := F_Q[\hat{\rho}, \hat{J}_\mathbf{n}] - F_{\text{SN}}[\hat{J}_\mathbf{n}]$ . The advantage is indeed bounded for  $(w, h)$ -separable states by

$$Q[\hat{\rho}_{(w,h)\text{-sep}}, \hat{J}_\mathbf{n}] \leq w(N - h). \quad (3)$$

A sensitivity that exceeds the shot-noise limit beyond this bound consequently implies metrologically useful  $(w, h)$ -entanglement.

We recover known bounds that only provide information on either  $w$  or  $h$  by ignoring part of the information contained in (2). For instance, by replacing  $h$  with the trivial lower bound  $N/w$ , we obtain the well-known sensitivity limit of  $w$ -producible states [11]

$$F_Q[\hat{\rho}_{w\text{-prod}}, \hat{J}_{\mathbf{n}}] \leq wN, \quad (4)$$

where  $1 \leq w \leq N$ . The result (2) thus generalizes (4) which has enabled the widespread study of multiparticle entanglement in quantum metrology [8], but also provides a valuable tool to understand entanglement in quantum-many body systems [2,4] and topological quantum phase transitions [23]. Similarly, we can ignore the information about  $w$  by using the trivial upper bound  $N - h + 1$ , yielding the sensitivity limit of  $h$ -separable states [24]

$$F_Q[\hat{\rho}_{h\text{-sep}}, \hat{J}_{\mathbf{n}}] \leq (N - h + 1)^2 + h - 1, \quad (5)$$

where  $1 \leq h \leq N$ .

Rather than fully ignoring the information provided by either  $w$  or  $h$ , we combine both into a more informative integer quantifier of multipartite entanglement. Dyson's rank  $r = w - h$  reflects the increase of correlations due to both larger  $w$  and smaller  $h$ . The range of  $r$  are the integer values from  $-(N - 1)$  to  $N - 1$  except  $\pm(N - 2)$  [14]. The set of states with Dyson's rank not larger than  $r$  is defined as  $\hat{\rho}_{r\text{-mk}} = \sum_{\Lambda \in \mathcal{L}_{r\text{-mk}}} P_{\Lambda} \hat{\rho}_{\Lambda}$  via the set  $\mathcal{L}_{r\text{-mk}} = \{\Lambda \mid \max \Lambda - |\Lambda| \leq r\}$  [13]. We obtain the bound [20]

$$F_Q[\hat{\rho}_{r\text{-mk}}, \hat{J}_{\mathbf{n}}] \leq \frac{(N + r)^2}{4} - \frac{1}{4} + N, \quad (6)$$

for all values of  $r$ , except for  $r = 4 - N$ , where we have  $F_Q[\hat{\rho}_{(4-N)\text{-mk}}, \hat{J}_{\mathbf{n}}] \leq N + 4$ . The first term in (6) clearly identifies the quadratic quantum advantage over the shot-noise limit offered by states with larger Dyson's rank  $r$  in terms of  $Q[\hat{\rho}, \hat{J}_{\mathbf{n}}]$ .

The upper bounds for  $(w, h)$ -separable states given in Eq. (2) are represented as a function of  $w$  and  $h$  in Fig. 2(a) [25]. The bounds on producibility (4) and separability (5) are recovered as the projections onto the axes describing  $w$  or  $h$  (red and green plots, respectively). Since these correspond to the short arms of the right triangle (blue columns) that is occupied by tuples  $(w, h)$ , these projections ignore large amounts of information on the respective other coordinate. A finer resolution can be obtained by the projection along the hypotenuse that is described by  $r = w - h$ . The most detailed information about multipartite entanglement is provided by the tuples  $(w, h)$ .

*Analysis of experimental data.*—Our results allow us to extract information about these quantities directly from  $F_Q$  without the need for additional measurements. To illustrate the power of this technique, we study the separability structure of experimentally generated quantum states based

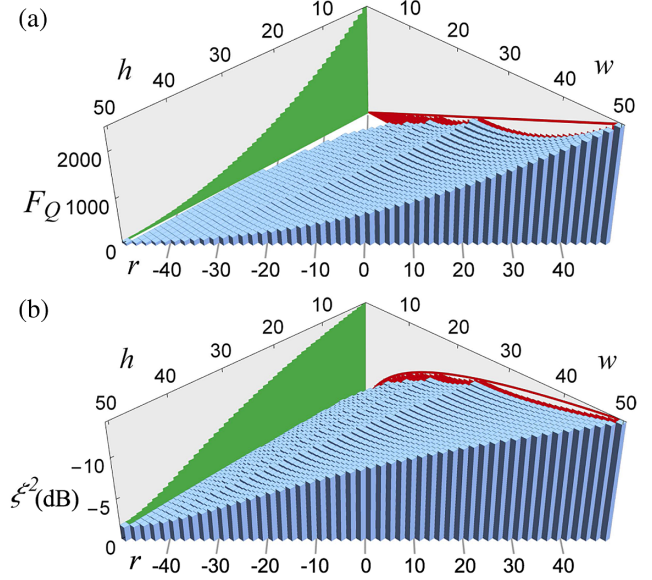


FIG. 2. Maximal metrological sensitivity for  $(w, h)$ -separable states as a function of  $w$  and  $h$ . The sensitivity limits are given for (a) the quantum Fisher information  $F_Q[\hat{\rho}, \hat{J}_{\mathbf{n}}]$  and (b) the spin-squeezing parameter  $\xi^2$ . By ignoring either  $w$  or  $h$ , we obtain bounds for  $w$ -producible (red projection) and  $h$ -separable states (green projection), respectively. A finer projection is given by Dyson's rank  $r = w - h$  [25].

on published lower bounds for  $F_Q$ . We first focus on an example with moderate particle number  $N = 14$ , reported in Ref. [26]. In this trapped-ion experiment a quantum Fisher information of at least  $F_Q[\hat{\rho}, \hat{J}_{\mathbf{z}}] \geq 40.4$  has been observed [27]. The performance of the different bounds can be gauged by the number of separable  $(w, h)$  classes, i.e., tuples  $(w, h)$  that are excluded. Note that more than one partition may be compatible with a tuple  $(w, h)$ . From Eq. (4) and its sharper version [20], we find that the measured data is incompatible with partitions of width  $w \leq 3$ , implying an entanglement depth of  $w = 4$ , which excludes 16 tuples [Fig. 3(a)]. Similarly, from Eq. (5) we find  $h = 9$ , excluding the 11 tuples of the system into more than 10 parts [Fig. 3(b)]. Much more information is obtained by using the bound (2), which excludes a total of 24 separable tuples [Fig. 3(d)] [25]. Among all single integer quantifiers, Dyson's rank, obtained from (6) to be  $r = -3$ , detects the largest amount of 20 separable tuples [Fig. 3(c)] [25]. The excluded tuples for each criterion are summarized in Fig. 3(e), where we also highlight specific inseparable partitions that remain undetected by the individual information on  $w$  or  $h$ .

This technique may also be applied to systems with larger particle numbers, as we illustrate through the analysis of additional data on measurements of lower bounds on the quantum Fisher information in systems of cold atoms and ions published in Refs. [26,28,29]. While for a full account, we refer to the Supplemental Material [20]; in Fig. 4(a) we show results obtained from the



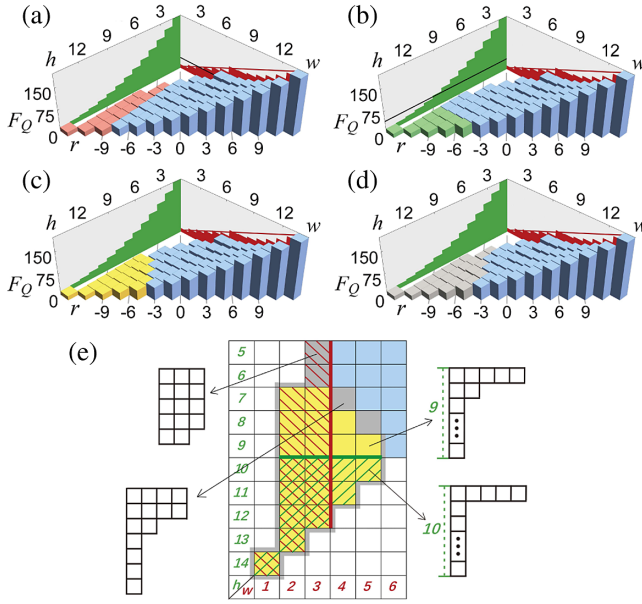


FIG. 3. Tuples  $(w, h)$  whose separability can be excluded from the experimentally extracted value of  $F_Q \geq 40.4$  for  $N = 14$  parties in Ref. [26] are highlighted. The red tuples (a) are excluded from the entanglement depth (4), the green tuples (b) from  $h$ -separability (5) and the yellow tuples (c) from Dyson's rank (6). The gray tuples (d) are found inseparable by Eq. (2), that uses the full information on  $(w, h)$  [25]. The results are summarized in the top-view plot (e), where each square represents one tuple  $(w, h)$  and example partitions with given width  $w$  and height  $h$  are illustrated.

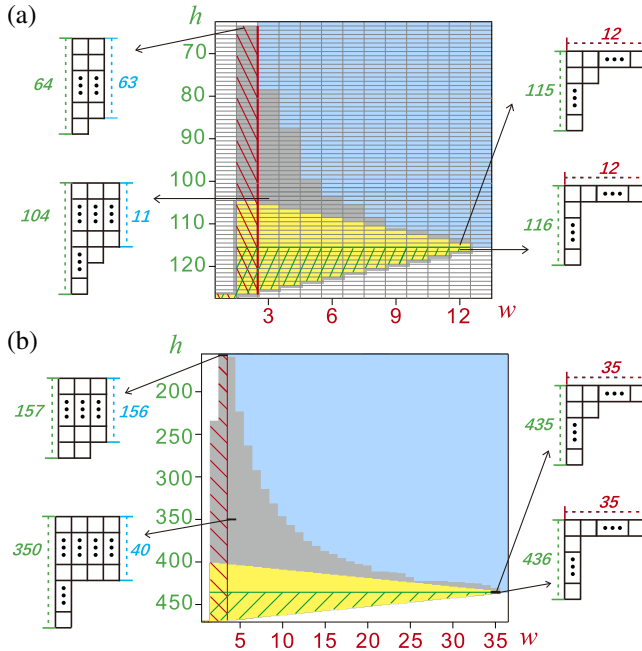


FIG. 4. (a) Analysis of the multipartite entanglement structure [same as in Fig. 3(e)] for  $N = 127$  parties based on the measurement of  $F_Q[\hat{\rho}, \hat{J}_z] \geq 266.7$  reported in Ref. [29]. (b) Same analysis based on the spin-squeezing coefficient (7) for a measurement of  $\xi^2 \leq -4.5$  dB with  $N = 470$  particles [17].

measurement of  $F_Q[\hat{\rho}, \hat{J}_z] \geq 266.7$  with  $N = 127$  trapped ions, as announced in Ref. [29]. Generally, we find that  $r$  is the most sensitive single integer quantifier of multipartite entanglement in the experimentally most relevant regime of finite entanglement. Only close to the limit of genuine multipartite entanglement, the entanglement depth  $w$  becomes slightly more sensitive than  $r$ , while at no point do we gain more information from  $h$  [20].

*Bounds for the spin-squeezing coefficient.*—We have so far focused on metrological entanglement witnesses that make use of the quantum Fisher information, the ultimate sensitivity limit achievable by an optimal measurement. In many experimental situations, it is more convenient to study the precision with respect to the specific measurement of a collective spin observable. This is achieved by spin-squeezing coefficients [8,30,31], first introduced by Wineland *et al.* as  $\xi^2 = N(\Delta\hat{J}_n)^2 / \langle \hat{J}_m \rangle^2$ , with suitably chosen, orthogonal directions  $\mathbf{n}$  and  $\mathbf{m}$  [30]. The spin-squeezing coefficient expresses the quantum gain in sensitivity over the shot-noise limit due to squeezing of a spin observable  $\hat{J}_n$  and has found widespread application in experiments with atomic systems [8]. Spin squeezing further gives rise to lower bounds on the quantum Fisher information [9,32] and provides an experimentally convenient witness for the entanglement depth  $w$  [7,22,33,34]. We derive state-independent bounds on  $\xi^2$  that are sensitive to both  $w$  and  $h$ , by relating the spin-squeezing coefficient to the bounds that we found for the quantum Fisher information. Specifically, we show that [20]

$$N \max_{\hat{\rho}_{\Lambda\text{-sep}}} \xi_{\hat{\rho}_{\Lambda\text{-sep}}}^{-2} \leq \frac{1}{2} \max_{\hat{\rho}_{\Lambda\text{-sep}}} F_Q[\hat{\rho}_{\Lambda\text{-sep}}, \hat{J}_n] + N, \quad (7)$$

which allows us to use our results (2), (4), (5), and (6) on  $F_Q$  to identify limits on  $\xi^2$  as a function of  $w$ ,  $h$ , or  $r$  [20]. These bounds are shown in Fig. 2(b). For instance, from Eq. (6) we obtain the limit

$$\xi_{\hat{\rho}_{r\text{-mk}}}^2 \geq \frac{8N}{(N+r)^2 + 12N - 1} \quad (8)$$

for states with Dyson's rank no larger than  $r$ . In Fig. 4(b) we summarize the entanglement analysis based on the experimentally measured value of  $\xi^2 \leq -4.5$  dB of spin squeezing for  $N = 470$  particles, reported in Ref. [17].

From the widely available experimental data on  $\xi^2$  and  $F_Q$ , we can immediately extract measured values of Dyson's rank  $r$  using the bounds (6) and (8) [25]. In Fig. 5 we analyze experimental data of Refs. [8,17,26–29,35–46], describing experiments with trapped ions, Bose-Einstein condensates and cold thermal atoms. In order to be able to compare the measurements with different numbers of particles  $N$ , we plot  $r + N$  with values in the range  $[1, 2N - 1]$ .

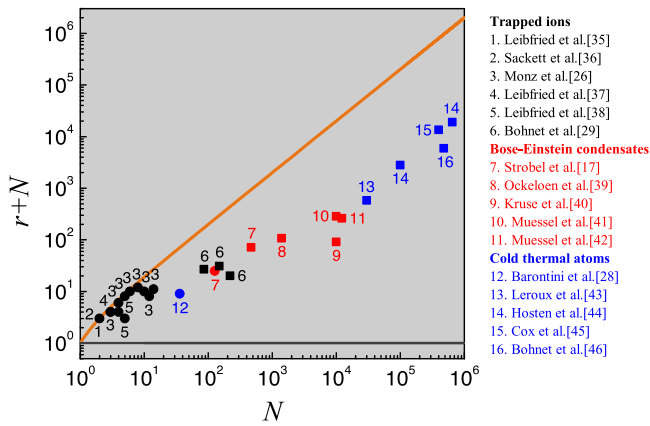


FIG. 5. Dyson's rank  $r$  as a function of  $N$  extracted from published experimental data on the spin-squeezing coefficient  $\xi^2$  (squares) or the quantum Fisher information  $F_Q$  (circles) based the results reported in Refs. [8,17,26–29,35–46]. The quantity  $r + N$  ranges between 1 for fully separable states (black line) and  $2N - 1$  for genuine  $N$ -partite entangled states (orange line).

**Conclusions.**—Based on widely used quantifiers for metrological sensitivity, we have derived entanglement witnesses that are sensitive to combined constraints on the size  $w$  of the largest entangled group ( $w$ -producibility or entanglement depth) and the number  $h$  of separable groups ( $h$ -separability). The description of inseparable partitions in terms of Young diagrams has allowed us to gain a precise understanding of metrologically useful multipartite entanglement beyond the information that can be provided by either  $w$  or  $h$  individually. Our techniques can be readily implemented for the theoretical and experimental study of multipartite entanglement in quantum information and many-body physics.

This research was supported by the National Key R&D Program of China (Grant No. 2017YFA0304500), National Natural Science Foundation of China (Grant No. 11874247), 111 project (Grant No. D18001), the Hundred Talent Program of the Shanxi Province (2018), and by the LabEx ENS-ICFP: ANR-10-LABX-0010/ANR-10-IDEX-0001-02 PSL\*.

\*wdli@sxu.edu.cn

†augusto.smerzi@ino.it

‡manuel.gessner@ens.fr

- [1] L. Amico, R. Fazio, A. Osterloh, and V. Vedral, Entanglement in many-body systems, *Rev. Mod. Phys.* **80**, 517 (2008).
- [2] P. Hauke, M. Heyl, L. Tagliacozzo, and P. Zoller, Measuring multipartite entanglement through dynamic susceptibilities, *Nat. Phys.* **12**, 778 (2016).
- [3] I. Frérot and T. Roscilde, Reconstructing the quantum critical fan of strongly correlated systems using quantum correlations, *Nat. Commun.* **10**, 577 (2019).
- [4] M. Gabbriellini, L. Lepori, and L. Pezzè, Multipartite-entanglement tomography of a quantum simulator, *New J. Phys.* **21**, 033039 (2019).

- [5] O. Gühne and G. Tóth, Entanglement detection, *Phys. Rep.* **474**, 1 (2009).
- [6] N. Friis, G. Vitagliano, M. Malik, and M. Huber, Entanglement certification from theory to experiment, *Nat. Rev. Phys.* **1**, 72 (2019).
- [7] G. Tóth and I. Apellaniz, Quantum metrology from a quantum information science perspective, *J. Phys. A* **47**, 424006 (2014).
- [8] L. Pezzè, A. Smerzi, M. K. Oberthaler, R. Schmied, and P. Treutlein, Quantum metrology with nonclassical states of atomic ensembles, *Rev. Mod. Phys.* **90**, 035005 (2018).
- [9] L. Pezzè and A. Smerzi, Entanglement, Nonlinear Dynamics, and the Heisenberg Limit, *Phys. Rev. Lett.* **102**, 100401 (2009).
- [10] V. Giovannetti, S. Lloyd, and L. Maccone, Advances in quantum metrology, *Nat. Photonics* **5**, 222 (2011).
- [11] P. Hyllus, W. Laskowski, R. Krischek, C. Schwemmer, W. Wieczorek, H. Weinfurter, L. Pezzè, and A. Smerzi, Fisher information and multiparticle entanglement, *Phys. Rev. A* **85**, 022321 (2012); G. Tóth, Multipartite entanglement and high-precision metrology, *Phys. Rev. A* **85**, 022322 (2012).
- [12] M. Gessner, L. Pezzè, and A. Smerzi, Sensitivity Bounds for Multiparameter Quantum Metrology, *Phys. Rev. Lett.* **121**, 130503 (2018).
- [13] S. Szalay,  $k$ -stretchability of entanglement, and the duality of  $k$ -separability and  $k$ -producibility, *Quantum* **3**, 204 (2019).
- [14] F. J. Dyson, Some guesses in the theory of partitions, *Eureka (Cambridge)* **8**, 10 (1944).
- [15] S. L. Braunstein and C. M. Caves, Statistical Distance and the Geometry of Quantum States, *Phys. Rev. Lett.* **72**, 3439 (1994).
- [16] V. Giovannetti, S. Lloyd, and L. Maccone, Quantum Metrology, *Phys. Rev. Lett.* **96**, 010401 (2006).
- [17] H. Strobel, W. Muessel, D. Linnemann, T. Zibold, D. B. Hume, L. Pezzè, A. Smerzi, and M. K. Oberthaler, Fisher information and entanglement of non-Gaussian spin states, *Science* **345**, 424 (2014).
- [18] M. Gessner, L. Pezzè, and A. Smerzi, Efficient entanglement criteria for discrete, continuous, and hybrid variables, *Phys. Rev. A* **94**, 020101(R) (2016).
- [19] Z. Qin, M. Gessner, Z. Ren, X. Deng, D. Han, W. Li, X. Su, A. Smerzi, and K. Peng, Characterizing the multipartite continuous-variable entanglement structure from squeezing coefficients and the Fisher information, *npj Quantum Inf.* **5**, 3 (2019); M. Gessner, L. Pezzè, and A. Smerzi, Entanglement and squeezing in continuous-variable systems, *Quantum* **1**, 17 (2017).
- [20] See Supplemental Material at <http://link.aps.org/supplemental/10.1103/PhysRevLett.126.080502> for details on the derivation of the separability limits on the quantum Fisher information, the spin-squeezing coefficient, as well as additional details on the analysis of experimental data, which contains additional Refs. [21,22].
- [21] L. Pezzè and A. Smerzi, Quantum theory of phase estimation, in *Atom Interferometry, Proceedings of the International School of Physics "Enrico Fermi", Course 188, Varenna*, edited by G. M. Tino and M. A. Kasevich (IOS Press, Amsterdam, 2014), p. 691.
- [22] M. Fadel and M. Gessner, Relating spin squeezing to multipartite entanglement criteria for particles and modes, *Phys. Rev. A* **102**, 012412 (2020).

- [23] L. Pezzè, M. Gabbriellini, L. Lepori, and A. Smerzi, Multipartite Entanglement in Topological Quantum Phases, *Phys. Rev. Lett.* **119**, 250401 (2017).
- [24] Y. Hong, S. Luo, and H. Song, Detecting  $k$ -nonseparability via quantum Fisher information, *Phys. Rev. A* **91**, 042313 (2015).
- [25] In the plots and analysis of experimental data, we use slightly stronger versions of the bounds (2), (4), (6), and (8) that are obtained by considering the division of  $N$  into integer subsets. The exact expressions and their derivation are provided in Ref. [20]. The red line in the projection of  $w$  represents the bound (4).
- [26] T. Monz, P. Schindler, J. T. Barreiro, M. Chwalla, D. Nigg, W. A. Coish, M. Harlander, W. Hänsel, M. Hennrich, and R. Blatt, 14-Qubit Entanglement: Creation and Coherence, *Phys. Rev. Lett.* **106**, 130506 (2011).
- [27] L. Pezzè, Y. Li, W. Li, and A. Smerzi, Witnessing entanglement without entanglement witness operators, *Proc. Natl. Acad. Sci. U.S.A.* **113**, 11459 (2016).
- [28] G. Barontini, L. Hohmann, F. Haas, J. Estève, and J. Reichel, Deterministic generation of multiparticle entanglement by quantum Zeno dynamics, *Science* **349**, 1317 (2015).
- [29] J. G. Bohnet, B. C. Sawyer, J. W. Britton, M. L. Wall, A. M. Rey, M. Foss-Feig, and J. J. Bollinger, Quantum spin dynamics and entanglement generation with hundreds of trapped ions, *Science* **352**, 1297 (2016).
- [30] D. J. Wineland, J. J. Bollinger, W. M. Itano, and D. J. Heinzen, Squeezed atomic states and projection noise in spectroscopy, *Phys. Rev. A* **50**, 67 (1994).
- [31] J. Ma, X. Wang, C. Sun, and F. Nori, Quantum spin squeezing, *Phys. Rep.* **509**, 89 (2011).
- [32] M. Gessner, A. Smerzi, and L. Pezzè, Metrological Non-linear Squeezing Parameter, *Phys. Rev. Lett.* **122**, 090503 (2019).
- [33] A. Sørensen, L. M. Duan, J. I. Cirac, and P. Zoller, Many-particle entanglement with Bose-Einstein condensates, *Nature (London)* **409**, 63 (2001).
- [34] A. S. Sørensen and K. Mølmer, Entanglement and Extreme Spin Squeezing, *Phys. Rev. Lett.* **86**, 4431 (2001).
- [35] D. Leibfried, B. DeMarco, V. Meyer, D. Lucas, M. Barrett, J. Britton, W. M. Itano, B. Jelenkovic, C. Langer, T. Rosenband, and D. J. Wineland, Experimental demonstration of a robust, high-fidelity geometric two ion-qubit phase gate, *Nature (London)* **422**, 412 (2003).
- [36] C. A. Sackett, D. Kielpinski, B. E. King, C. Langer, V. Meyer, C. J. Myatt, M. Rowe, Q. A. Turchette, W. M. Itano, D. J. Wineland, and C. Monroe, Experimental entanglement of four particles, *Nature (London)* **404**, 256 (2000).
- [37] D. Leibfried, M. D. Barrett, T. Schaetz, J. Britton, J. Chiaverini, W. M. Itano, J. D. Jost, C. Langer, and D. J. Wineland, Toward Heisenberg-Limited spectroscopy with multiparticle entangled states, *Science* **304**, 1476 (2004).
- [38] D. Leibfried, E. Knill, S. Seidelin, J. Britton, R. B. Blakeshtad, J. Chiaverini, D. B. Hume, W. M. Itano, J. D. Jost, C. Langer, R. Ozeri, R. Reichle, and D. J. Wineland, Creation of a six-atom ‘Schrödinger cat’ state, *Nature (London)* **438**, 639 (2005).
- [39] C. F. Ockeloen, R. Schmied, M. F. Riedel, and P. Treutlein, Quantum Metrology with a Scanning Probe Atom Interferometer, *Phys. Rev. Lett.* **111**, 143001 (2013).
- [40] I. Kruse, K. Lange, J. Peise, B. Lücke, L. Pezzè, J. Arlt, W. Ertmer, C. Lisdat, L. Santos, A. Smerzi, and C. Klempt, Improvement of an Atomic Clock Using Squeezed Vacuum, *Phys. Rev. Lett.* **117**, 143004 (2016).
- [41] W. Muessel, H. Strobel, D. Linnemann, D. B. Hume, and M. K. Oberthaler, Scalable Spin Squeezing for Quantum-Enhanced Magnetometry with Bose-Einstein Condensates, *Phys. Rev. Lett.* **113**, 103004 (2014).
- [42] W. Muessel, H. Strobel, D. Linnemann, T. Zibold, B. Juliá-Díaz, and M. K. Oberthaler, Twist-and-turn spin squeezing in Bose-Einstein condensates, *Phys. Rev. A* **92**, 023603 (2015).
- [43] I. D. Leroux, M. H. Schleier-Smith, and V. Vuletić, Implementation of Cavity Squeezing of a Collective Atomic Spin, *Phys. Rev. Lett.* **104**, 073602 (2010).
- [44] O. Hosten, N. J. Engelsen, R. Krishnakumar, and M. A. Kasevich, Measurement noise 100 times lower than the quantum-projection limit using entangled atoms, *Nature (London)* **529**, 505 (2016).
- [45] K. C. Cox, G. P. Greve, J. M. Weiner, and J. K. Thompson, Deterministic Squeezed States with Collective Measurements and Feedback, *Phys. Rev. Lett.* **116**, 093602 (2016).
- [46] J. G. Bohnet, K. C. Cox, M. A. Norcia, J. M. Weiner, Z. Chen, and J. K. Thompson, Reduced spin measurement back-action for a phase sensitivity ten times beyond the standard quantum limit, *Nat. Photonics* **8**, 731 (2014).